The LINNEAN SOCIETY of London BIOLOGICAL Journal of the Linnean Society

Biological Journal of the Linnean Society, 2016, ••, ••–••. With 1 figure.

Phylogeography and population structure of two *Brachistosternus* species (Scorpiones: Bothriuridae) from the Chilean coastal desert – the perils of coastal living

F. SARA CECCARELLI[1]*, JAIME PIZARRO-ARAYA[2] and ANDRÉS A. OJANGUREN-AFFILASTRO[1]

[1]*División de Aracnología, Museo Argentino de Ciencias Naturales "Bernardino Rivadavia", Av. Ángel Gallardo 470, C1405DJR, Buenos Aires, Argentina*
[2]*Laboratorio de Entomología Ecológica, Departamento de Biología, Facultad de Ciencias, Universidad de La Serena, Casilla 599, La Serena, Chile*

Received 2 May 2016; revised 22 June 2016; accepted for publication 22 June 2016

Coastal deserts are geologically dynamic areas of the Earth, affected by historical changes in sea levels and in some cases also by fault-line tectonic activity. An example of such a dynamic area is the Chilean coastal desert of the Antofagasta and Atacama regions, which harbours many endemic species, such as the bothriurid scorpion species *Brachistosternus paposo* and *Brachistosternus roigalsinai*. In this work, we carry out phylogeographic and population genetic analyses on these scorpions, using two mitochondrial (COI and cyt *b*) and two nuclear (Actin 5C and wingless) markers to identify species and population structuring, and link these findings to the geological history of the area. The geographical feature separating the two species is identified as the Huasco River, and distinguishing morphological features for these scorpions are presented. Population genetic and phylogeographic outcomes reflect an unstable history across this region for *B. paposo* and *B. roigalsinai*, related to sea-level changes affecting coastal habitats, including nearby islands. © 2016 The Linnean Society of London, *Biological Journal of the Linnean Society*, 2016, **00**, 000–000.

KEYWORDS: Chile – eustasy – population genetics – vicariant speciation.

INTRODUCTION

The desert biome covers about one-fifth of the world's terrestrial surface and is characterised by extreme environments in which only organisms with specific adaptations can survive (Mulroy & Rundel, 1977; Whitford, 2002; Nagy, 2004). Deserts also provide spatiotemporal habitat stability for well adapted species (Hartley *et al.*, 2005). Coastal deserts, however, are an exception to this stability over time, as their geographical areas are prone to changes depending on global sea levels, or eustasy (Carter, 1988). While global sea levels during the late Neogene and Quaternary periods have been estimated to oscillate by more than 150 m (Haq, Hardenbol & Vail, 1988; Hardenbol *et al.*, 1998), the shorelines and their features have been shaped by a combination of sea-level changes and tectonics (Pedoja *et al.*, 2014). This means that, since the Pliocene, low-lying regions of present-day coastal areas (including low-elevation islands) have been submerged numerous times and areas with a shallow sea floor have repeatedly emerged, thus also joining coastal-shelf islands to the mainland.

The South American Pacific Coastal Desert (PCD) of Chile and Peru is an example of a dynamic geographical area with an extreme environment. The Chilean coastal desert extends from the Tarapacá to the Coquimbo region. The most important rivers found in this area are, from north to south, the Copiapó, Huasco, and the Elqui. The River Copiapó has a semi-permanent flow and is an endorheic system, meaning that it does not drain into the ocean, whereas the Huasco and Elqui rivers have a

*Corresponding author: E-mail: saracecca@hotmail.com

permanent flow draining into the Pacific Ocean, which makes them exorheic systems. This area also contains several continental-shelf islands. To the south is the Choros archipelago, which comprises the Choros, Damas, and Gaviota islands. The farthest from the continent is Choros, which is almost 8 km off the coast; next is Damas, about 5 km, and the closest is Gaviota, which is < 1 km off the coast; the sea floor between these islands and the coast does not drop below 30 m. Twenty-five km north of the Choros archipelago, is Chañaral island, located about 8 km off the coast with an intervening seafloor depth of about 80–120 m (Aguirre, 1967). Chañaral, Choros and Damas islands belong to the Pingüino de Humboldt National Reserve (Sistema Nacional de Áreas Silvestres Protegidas del Estado, SNASPE area; Castro & Brignardello, 2005; see Supporting Information, Figure S1 of the Supporting Information). Like several other coastal areas, this region has been affected by constant sea-level changes (Le Roux *et al.*, 2005) coupled with tectonic uplift and associated seismic activities caused by the subduction of the Nazca plate under the South American plate (Kendrick *et al.*, 2003; Husson, Conrad & Faccenna, 2012). Such geological events are expected to have affected the local flora and fauna populations as well.

Population genetic and phylogeographic analyses are useful tools for inferring past patterns and processes of species at the transition between intra- and inter-specific levels, which, in the case of extreme, geographically dynamic areas such as the Chilean coastal desert, reveal the extent to which this relative instability affects its inhabitants. Furthermore, the effect of geographic barriers (such as rivers and the sea separating islands from the mainland) on genetic structuring can be assessed.

Among the South American desert-specialized fauna, several scorpions belonging to the families Bothriuridae, Buthidae, and Caraboctonidae have adapted to living in this extreme environment. Particularly, the scorpion genus that is most adapted and diversified in these areas is *Brachistosternus*, belonging to the family Bothriuridae, which occurs even in the most extreme arid environments of the continent, such as the Atacama and Sechura deserts (Ochoa, 2005; Ojanguren-Affilastro & Ramírez, 2009; Kovařík & Ojanguren-Affilastro, 2013; Ceccarelli *et al.*, 2016; Ojanguren-Affilastro *et al.*, 2016). To date, scorpion phylogeographic and population genetic studies have been carried out on Holartic fauna of families such as Buthidae and Vaejovidae (e.g. Mirshamsi *et al.*, 2010; Graham, Oláh-Hemmings & Fet, 2012; Bryson, Savary & Prendini, 2013; Graham *et al.*, 2013), but never on Neotropical bothriurids.

One of the five major clades of the bothriurid scorpion genus *Brachistosternus*, named the Pacific Coastal Desert Clade (PCDC) (Ojanguren-Affilastro *et al.*, 2016), is found in the PCD, which is itself an area of high phylogenetic diversity for this genus (Ceccarelli *et al.*, 2016). The PCDC species migrated and speciated along the coast in a general northward direction, from an ancestral area on the central Chilean coast (Ceccarelli *et al.*, 2016). A sister group to the remaining PCDC species, *Brachistosternus paposo* (Ojanguren-Affilastro & Pizarro-Araya, 2014) and *Brachistosternus roigalsinai* (Ojanguren-Affilastro, 2002) inhabit a similar area of the Chilean coastal desert. No evidence for sympatry has been found so far in the two species (Ojanguren-Affilastro & Pizarro-Araya, 2014), with the geographical limits thought to be at 26° to 30° for *B. roigalsinai* (Ojanguren-Affilastro, Mattoni & Prendini, 2007a; Ojanguren-Affilastro *et al.*, 2007b), and restricted to the area of Paposo (approximately at 25°) for *B. paposo* (Ojanguren-Affilastro & Pizarro-Araya, 2014). Additionally, the presence of *B. roigalsinai* has also been reported from the Choros archipelago (Pizarro-Araya *et al.*, 2014a), and recently several specimens of this species have been collected from Chañaral island (Alfaro, Pizarro-Araya & Mondaca, 2014; Pizarro-Araya *et al.*, 2014b); however, the island specimens present slight morphological differences with respect to the continental populations, as was found for the tenebrionid *Praocis* (*Praocis*) *spinolai* (Benítez *et al.*, 2014). Based on the results of a recent molecular study (Ojanguren-Affilastro *et al.*, 2016), the distributional limits of the two species have been questioned, raising doubts about the diagnostic characters of both species and the specific identity of their populations.

Here, a more detailed study of the morphology of several populations of *B. roigalsinai* and *B. paposo* from their entire distributional range, combined with the data of the species delimitation analysis presented by Ojanguren-Affilastro *et al.* (2016), sheds light on the identity and diagnostic characters of these two species. Based on these newly inferred species limits, the phylogeography and population histories of two bothriurid scorpion species from the Chilean coastal desert, *B. paposo* and *B. roigalsinai* are investigated, to answer questions about speciation and population structure in extreme environments such as coastal deserts, and to link these historical microevolutionary processes with the area's geography and geological history. This project is the first phylogeographic and population genetic study involving bothriurid species, or even a Neotropical scorpion, applying a wide range of methods to obtain a full spectrum of structural, spatial and temporal genetic dynamics.

MATERIALS AND METHODS

SPECIES LIMITS AND DIAGNOSTIC CHARACTERS

Brachistosternus paposo and *B. roigalsinai* are considered two distinct valid species based on the species delimitation analyses of Ojanguren-Affilastro *et al.* (2016; Appendix H). All available specimens of both species (about 300 of *B. roigalsinai*, and 150 of *B. paposo*) were examined during this study to re-establish and evaluate the strength of a new morphological diagnostic characteristic, namely the presence of two dark spots in the posterodorsal margin of sternite VII and metasomal segments I–III of *B. roigalsinai*, which are absent in *B. paposo* (see Fig. 1).

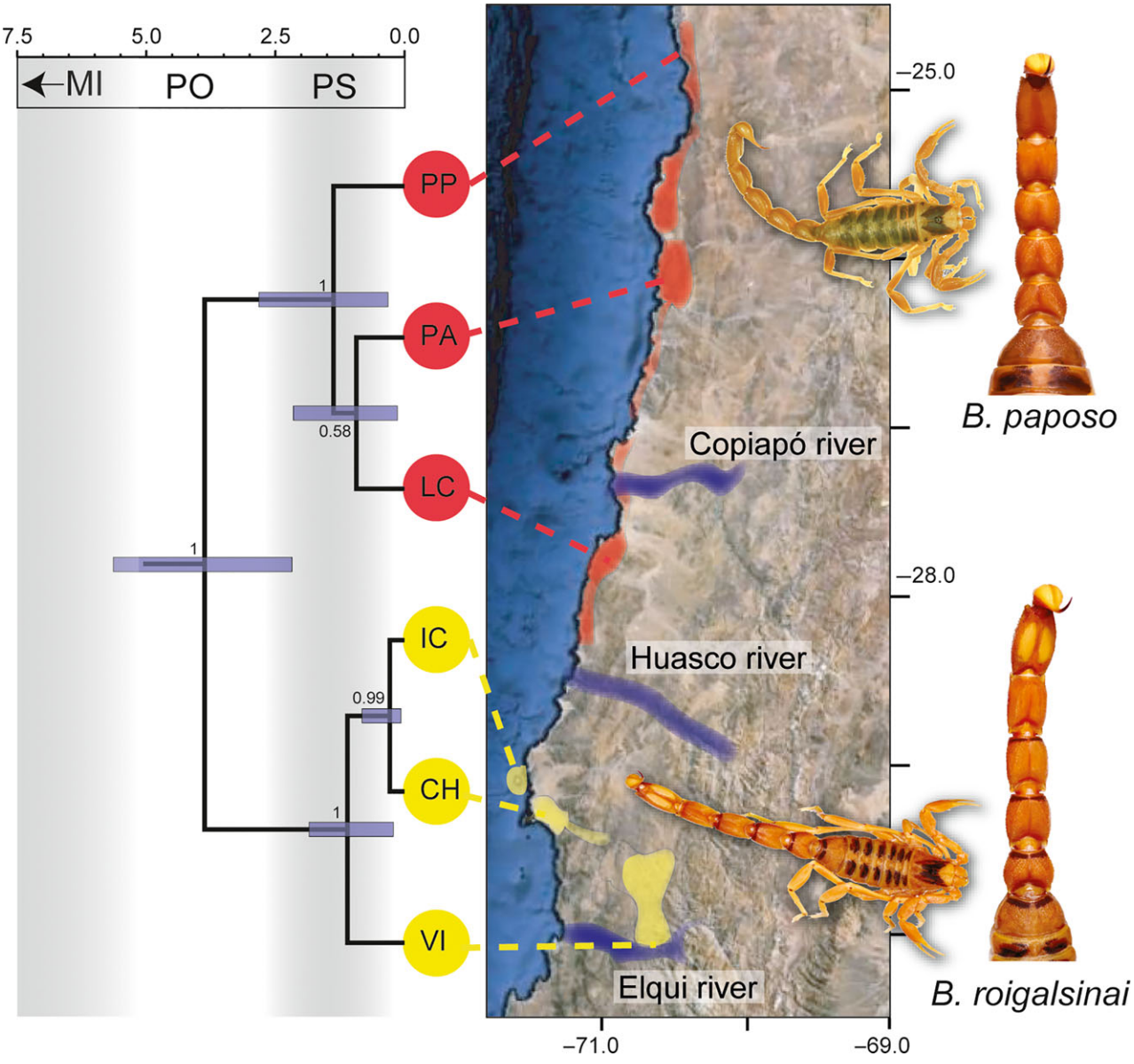

Figure 1. Coalescence-based ultrametric tree obtained from *BEAST using the nuclear actin and wingless, and mitochondrial COI and cyt *b* gene fragments, with populations as terminal taxa (for codes see Table 2). Upper bar with ages (in Myr) and geological epochs are shown above the tree (MI = Miocene; PO = Pliocene; PS = Pleistocene). Bayesian posterior probabilities are shown as numbers at nodes, and blue bars represent 95% highest posterior densities. Red circled terminal populations represent *Brachistosternus paposo* and yellow *Brachistosternus roigalsinai*, also shown on the map by approximated, respectively coloured polygons and adjoining dashed lines. The map in the centre also contains blue polygons marking the Copiapó, Huasco and Elquí river drainages. To the left of the map are photographs of male specimens of each species, each with an enlarged photograph of their respective metasomas to illustrate the difference in pigmentation.

Taxon sampling and molecular marker selection

To assess their population structure and phylogeographic histories, 56 individuals belonging to the nominal species *B. roigalsinai* and *B. paposo* were collected, 39 of which were collected from nine continental localities along the Chilean coastal desert between the latitudes 24°S and 31°S (see Table 1 and Supporting Information, Table S1 for details). An additional 17 specimens of *B. roigalsinai* were also included from three coastal islands of Atacama – more specifically, two localities of the Choros archipelago (the Choros and Damas islands) and one locality from Chañaral island. One individual of *Brachistosternus ochoai* Ojanguren-Affilastro, 2004 was used as an outgroup taxon for the tree inference (in BEAST, see section on COALESCENCE-BASED TREE INFERENCE below). The analyses were based on molecular data pertaining to two mitochondrial and two nuclear gene fragments in the form of DNA sequence data. The mitochondrial markers belonged to the cytochrome oxidase *C* subunit I (henceforth COI) and the cytochrome B (cyt *b*) gene fragments, while the nuclear markers belonged to the Actin 5C (actin) and wingless (wg) gene fragments. The nuclear markers, although never used for scorpions, have been employed for molecular phylogenetic studies in other arachnids (e.g. Vink *et al.*, 2008; Blackledge *et al.*, 2009; Bodner & Maddison, 2012) and to date there is no evidence for paralogues of these genes. Having said that, neither gene nor even whole-genome duplication for the scorpion species studied here has ever been investigated. Nevertheless, based on the number and distribution of the nuclear genes' heterozygous sites (see Results), the assumption of homology is reasonable.

Table 1. Sampling localities for the bothriurid scorpion species *Brachistosternus paposo* and *Brachistosternus roigalsinai* on the Chilean coast

Locality name	Loc. #	Latitude	Longitude
Paposo	1	−25.017212	−70.46711
Pan de Azúcar N.P.	2	−26.166975	−70.66353
Llanos de Challe N.P., inland	3	−28.118129	−71.09731
Llanos de Challe N.P., beach	4	−28.129638	−71.162081
Caleta Los Burros	5	−28.193802	−71.154944
Chañaral Island N.R.	6	−29.03388	−71.577658
Damas Island N.R.	7	−29.235708	−71.527106
Choros Island N.R.	8	−29.263887	−71.541684
Punta Choros, dunes	9	−29.243571	−71.434898
Choros inland 1	10	−29.322137	−71.233368
Choros inland 2	11	−29.337366	−71.224795
Vicuña	12	−30.028273	−70.722026

Locality number to cross-reference with Supporting Information, Figure S1; N.P. and N.R. in locality names refer to National Park and National Reserve, respectively.

DNA extraction, PCR and sequencing

Whole genomic DNA was extracted from leg muscle tissue of individual scorpions using a Qiagen DNeasy Blood and Tissue Kit, following the manufacturer's protocol and digesting the tissue at 56°C for 1 h with proteinase K. Polymerase chain reaction (PCR) mixes contained 1.5 μL 10× PCR Buffer (Life Sciences), 10 μmol $MgCl_2$, 0.25 μmol of each dNTP, 0.4 μmol of each primer, 0.1 μL *Taq* polymerase (5 U/μL, Life Sciences), 0.5 μL (50 mg/mL) bovine serum albumin, 1–2 μL genomic DNA and ddH_2O to bring the final volume to 15 μL. Four gene fragments (two mitochondrial and two nuclear) were amplified using the primers in Supporting Information (Table S2). All amplifications were performed using the following thermal profile: 94°C for 3–5 min; 35 cycles of 95°C for 15–30 s, 42–52°C for 15–30 s, 72°C for 15–30 s; 72°C for 10 min. The PCR products were purified using ExosAP (Life Sciences) and sent for sequencing to Macrogen Inc., Korea.

Data matrices handling and defining population limits

The DNA sequences of the partial COI, cyt *b*, actin and wg gene fragments were edited in Sequencher v. 4.1.4 (GeneCodes Corp.) and aligned in MAFFT 7 (Katoh & Standley, 2013) using the 'Auto' strategy and a gap opening penalty of 1.53. The COI and cyt *b* gene fragments were combined (henceforth referred to as the 'mt fragment') as mitochondrial markers are genetically linked. For the nuclear fragments, the PHASE algorithm (Stephens, Smith & Donnelly, 2001; Stephens & Donnelly, 2003) implemented in DnaSP v. 5.10.01 (Librado & Rozas, 2009) was used to separate heterozygous alleles, setting 1000 MCMC iterations (with a 10% burn-in) with the default settings for the 'Recombination' model, assuming no knowledge about the specific phases. Additionally, the nuclear fragments were checked for recombination in DnaSP, which computes the recombination parameter *R* (Hudson, 1987) and provides the minimum number of recombination events as calculated by the four-gamete test (Hudson & Kaplan, 1985). Sites containing missing data were removed and only the largest portion of the gene fragment free

from recombination was used, following a conservative approach.

To determine whether each sampled locality contained individuals that could be treated as separate populations, we used the Geneland v. 4.0.5 package (Guillot & Santos, 2009), running the Graphical User Interface in R v. 3.1.1 (R_core_team, 2014). Geneland uses MCMC sampling and a spatial model to estimate the number of populations and their geographic limits based on multilocus genotype data and GPS coordinate inputs. The number of populations was set between 1 and 10 and the analysis run for 10 million generations and a 10% burn-in, setting the spatial correlation between allele frequencies. To corroborate the results from Geneland, the program Structurama (Huelsenbeck & Andolfatto, 2007; Huelsenbeck, Andolfatto & Huelsenbeck, 2011) was used, running a Bayesian analysis under a Dirichlet probability distribution with a gamma shape parameter and assuming no admixture. The number of populations (k) was set between 1 and 10, and the program was run for four replicates of 10 million cycles with a 10% burn-in on the haplotype data from the PHASE analysis, coded as numbers.

Coalescence-based tree inference

Based on the previously inferred population limits, a coalescence-based analysis in *BEAST v. 1.8.2 (Heled & Drummond, 2010) was carried out to obtain a tree with one terminal per population with a reliable topology and node age estimates, as well as a set of posterior trees required for selected downstream analyses (see ISOLATION-WITH-MIGRATION and BAYESIAN PHYLOGEOGRAPHIC ANALYSES sections below). Due to difficulties with applying node age calibrations directly in *BEAST, the molecular substitution (or clock) rate for the mt fragment was estimated in BEAST v.1.8.2 (Drummond *et al.*, 2012), to be then used as a prior in the *BEAST analysis. The molecular rate was estimated based on a secondary calibration of *B. roigalsinai* and *B. paposo*'s divergence from their most recent common ancestor (set as a normal distribution prior with a mean of 6 Myr and 1.5 standard deviations), estimated to have occurred between 3.88 and 8.87 Mya (Ma; 95% HPD; Ceccarelli *et al.*, 2016). Partitioning strategies and nucleotide substitution models for the mt fragment were then selected using PartitionFinder v. 1.1.1 (Lanfear *et al.*, 2012) and an uncorrelated lognormal clock rate was set for each partition, linking the tree prior and setting it to a constant-size coalescent process. Two independent MCMC simulations of 50 million generations (sampling every 5000th) were run, checked for convergence (and ESS values of the parameters confirmed to be > 200) using Tracer v. 1.6 (Rambaut *et al.*, 2014), and the estimated mean and standard deviation of the clock rate for the two runs was noted.

For the *BEAST analysis on the mt and phased nuclear data, nucleotide substitution and clock model priors were unlinked, setting the partitions and nucleotide substitution models as chosen by PartitionFinder (see Supporting Information, Table S3). Uncorrelated lognormal relaxed clock priors were set for each molecular marker as a whole and the clock rate for the mitochondrial fragment was set using 0.0133 substitutions Myr^{-1}, based on the calibration obtained in BEAST. A Yule process tree prior was chosen and three separate MCMC runs of 20 million generations each were executed, sampling every 2000th generation. The convergence and ESS values of the runs were verified in Tracer and the trees combined in LogCombiner, removing the first 10% as burn-in, upon which the MCC tree with mean node heights was selected in TreeAnnotator. The BEAST and *BEAST analyses were run through the CIPRES Science Gateway bioinformatics portal v. 3.3 (Miller, Pfeiffer & Schwartz, 2010).

Population genetic parameter estimations

Based on the previously inferred population assignments, intra- and interpopulation genetic parameters were calculated in DnaSP on the complete COI and cyt *b* regions as well as on the non-recombining regions of actin and wg. More specifically, the intrapopulation genetic diversity was calculated based on the number of haplotypes (h), haplotype diversity (H), nucleotide diversity (π; Nei, 1987), and the Watterson parameter (θ; Watterson, 1975). Neutrality tests (Tajima's D [Tajima, 1989], Fu's F_S [Fu, 1997] and R_2 [Ramos-Onsins & Rozas, 2002]) were also carried out to test whether all of the populations adhere to the neutral hypothesis. The Z_{nS} (Kelly, 1997) values were calculated to infer the levels of linkage disequilibrium (LD). All of the parameters were calculated under the coalescent process (Hudson, 1990) and their statistical significance assessed through 10 000 simulated replicates.

The D_{xy} and D_a parameters (the average and net number of nucleotide substitutions per site between populations, respectively) were used to assess interpopulation genetic diversity levels, applying the Jukes and Cantor correction (Jukes & Cantor, 1969). Additionally, a neighbour-joining tree was estimated based on D_{xy} values for each marker separately using MEGA 6 (Tamura *et al.*, 2013). The levels of gene flow among the populations were assessed based on the N_{st} metric (Lynch & Crease, 1990) under the infinite island model (Wright, 1931).

For each population, the changes in population size over time were estimated by generating extended Bayesian skyline plots (EBSP; Heled & Drummond, 2008) in BEAST 1.8.2. Three data partitions were used: the mitochondrial fragment (COI + cyt *b*), the actin fragment and the non-recombining portion of the wg fragment. The linear EBSP coalescent tree prior was chosen for the linked partitions and an uncorrelated relaxed lognormal clock prior applied to each unlinked partition. Furthermore, the GTR nucleotide substitution model was chosen as a prior for the unlinked partitions and, for the demographic population size changes, a Poisson prior was applied. The MCMC chains were run for 20 million generations, sampling every 2000th generation. Graphs of population size changes over time were then generated from the output using Python scripts available online (https://code.google.com/archive/p/beast-mcmc/downloads).

Spatial population analyses

The program Alleles In Space (Miller, 2005) was used to detect potential barriers to gene flow across space (Manel *et al.*, 2003) by running an Allelic Aggregation Index Analysis, which quantifies the spatial patterns of individual haplotypes, setting 5000 randomised replicates. To help visualize the genetic distance patterns across the distributional range of *B. paposo* and *B. roigalsinai*, the program's 'Genetic Landscape Shape' interpolation was applied on a 50 × 100 grid, obtaining a landscape shape plot where the surface plot height represents genetic distance across space (Miller, 2005; Miller *et al.*, 2006). Further spatial visualisation, this time for haplotypes, was obtained by running a TCS (Templeton, Crandall & Sing, 1992) haplotype network analysis implemented in the program popART (Leigh & Bryant, 2015), which also facilitates visualization of haplotype representations on a map. Lastly, the regression significance of the previously calculated pairwise genetic distances (D_{xy}) was evaluated and isolation by distance tested, using a Mantel test (Mantel, 1967) with 30 000 randomizations for the natural log-transformed geographical distances provided by the Isolation By Distance Web Service (Jensen, Bohonak & Kelley, 2005).

Isolation-with-migration analyses

To determine the extent of genetic interchange between the populations of this study, current and historical migration rates and gene flow were assessed using Bayesian analyses in both the migrate-n v. 3.6.11 (Beerli, 2006, 2009) and the IMa2 (Hey & Nielsen, 2007; Hey, 2010) programs, as independent estimates of similar parameters. Migrate-n was run through the CIPRES Science Gateway on the nuclear and mitochondrial sequence data separately for all populations together and running four MCMC simulations for 50 million generations each with chain-swap and heating implemented (temperatures at 1, 1.5, 3, and 1 million, as per the default settings). Migration was confined to occur between geographically neighbouring populations, with starting θ and migration rates set to be calculated by the program and default settings used for the remaining parameters.

For IMa2, separate runs were executed for *Brachistosternus paposo* and *B. roigalsinai* populations, setting the input topologies for the populations as inferred by *BEAST, in each case combining mitochondrial and nuclear DNA data while providing the inheritance scalar (0.25 for the mtDNA as compared with the nucDNA). In the absence of known generation times for these scorpions, the value was set at 3, an average value for commonly known generation times in scorpions (e.g. Polis & Farley, 1980; Boulton & Polis, 1990; Polis, 1990), and the option of adding an unsampled 'ghost' population was activated. Four separate MCMC runs of 1 million generations were executed for each species to compare ESS values and chain mixing. For each run, 60 chains were set with heating terms of 0.975 and 0.75, and the uniform priors for the migration, population size and splitting time were set at maximum values of 5 each upon revising the histograms of preliminary runs. The Nielsen & Wakeley (2001) likelihood ratio test implemented in IMa2 was used to assess significant levels of migration.

Bayesian phylogeographic analysis

Bayesian phylogeographic analyses combine both spatial and temporal information to trace the most probable movements of populations through space and time. A relaxed random walk (RRW) Bayesian phylogeographic approach (Lemey *et al.*, 2010) was therefore used to infer the movements of *B. roigalsinai* and *B. paposo* populations across geographic space through time. The approach developed by Nylinder *et al.* (2014) was applied using the program BEAST v. 1.8.2. For this approach, the last 2000 species trees from the *BEAST analysis described earlier were used, after pruning the outgroup taxon in Mesquite v. 3.04 (Maddison & Maddison, 2015). Google Earth v. 7.1.5 was used to create polygons of the approximate extant distributions for each population, and used with the posterior distribution of species trees for the species-tree diffusion analysis under the RRW process. Following Nylinder *et al.* (2014), the same priors were used, including a prior exponential

distribution on the standard deviation of the lognormal distribution with a mean of 2.712. Four independent replicates of the species-tree diffusion analysis were run for 50 million generations each, logging every 50 000 generations. To visualise the ancestral 80% HPD regions in Google Earth at 1000 year intervals from 4.15 to 0 Mya, the 'time slice' function of the program SPREAD v. 1.0.6 (Bielejec *et al.*, 2011) was used on the output of the RRW species diffusion analysis.

RESULTS

Data matrices and coalescence-based tree inference

The details for the data matrices of the COI, cyt *b*, actin, and wg gene fragments used in this study can be found in Supporting Information (Table S4). Prior to their reduction based on inferred recombination events, the nuclear gene fragments, actin and wingless, contained no polymorphic sites for 24/34 and 22/51 (homozygous) individuals, respectively. Furthermore, seven and 19 individuals contained only one dimorphic site for actin and wingless, respectively. The maximum number of dimorphic sites for a single individual was three for actin and four for wingless. No individual had more than two nucleotidic variants at one site for either marker.

Based on the *BEAST tree inference, a clear separation is noted between the three populations of *Brachistosternus paposo* and *B. roigalsinai* (see Fig. 1). Age estimates were of 4.06 Ma (2.5–5.58 95% HPD) for the MRCA of the species *B. paposo* and *B. roigalsinai*, and of 1.36 Ma (0.32–2.84 95% HPD) and 1.27 Ma (0.22–2.52 95% HPD) for the MRCAs of the *B. paposo* and *B. roigalsinai* populations, respectively.

Population dynamics

The analyses carried out in Geneland and Structurama to estimate the number of populations both recovered five populations from the 12 sampled localities (see Supporting Information, Figures S2 and S3). Even though the individuals from Paposo (Loc 1) and Pan de Azúcar National Park (Loc 2) were grouped together, we decided to treat them as distinct populations for subsequent analyses since they are separated by more than 120 km. The final population assignment by locality can be found in Table 2.

For the intrapopulation DNA sequence variation and neutrality tests, the calculated values are presented in Supporting Information (Table S5). For Tajima's *D*, negative values were obtained for all populations and all markers, Fu's *Fs* values were all positive, but non-significant, while R_2 values were significantly different than expected under a neutral model. Similarly, significant results were obtained for all markers and populations for the Z_{nS} statistic measuring LD.

Table 2. Population assignments for *Brachistosternus paposo* and *Brachistosternus roigalsinai* based on Geneland and Structurama results

Species	Locality name	Loc nr.	Population code
B. paposo	Paposo	1	PP
B. paposo	Pan de Azúcar N.P.	2	PA
B. paposo	Llanos de Challe N.P., inland	3	LC
B. paposo	Llanos de Challe N.P., beach	4	LC
B. paposo	Caleta Los Burros	5	LC
B. roigalsinai	Chañaral Island N.R.	6	IC
B. roigalsinai	Damas Island N.R.	7	CH
B. roigalsinai	Choros Island N.R.	8	CH
B. roigalsinai	Punta Choros, dunes	9	CH
B. roigalsinai	Choros inland 1	10	CH
B. roigalsinai	Choros inland 2	11	CH
B. roigalsinai	Vicuña	12	VI

N.P. and N.R. in locality names refer to National Park and National Reserve, respectively.

The results of the F_{st} and D_{xy}/D_a calculations, used to determine structuring within vs. structuring between populations, are shown in Supporting Information (Table S6). The lowest structuring was found between populations of *B. roigalsinai* of Chañaral island (IC) and the Choros region (CH; Choros island and Punta Choros) based on the mitochondrial and wingless gene fragments, while based on these same two markers, there is genetic structuring between the northern populations of *B. paposo* (Paposo [PP], Pan de Azúcar National Park [PA] and Llanos de Challe National Park [LC]) and the coastal populations of *B. roigalsinai* of Chañaral island/Choros region. The actin fragment appears to confound this general pattern. A graphical representation of genetic structuring (or lack thereof) for each marker can be found in the neighbour-joining trees from the D_{xy} calculations in Supporting Information, Figure S4.

The extended Bayesian skyline plots (EBSP) for the different populations show no change in population size (LC and PA) or a slight increase (PP) during the last 50 000 years (50 kyr) for *B. paposo*. In

the case of *B. roigalsinai*, no genetic variation was found in the population from IC, meaning that an EBSP could not be obtained. Conversely, the populations from CH and VI showed slight and considerable population growth, respectively, especially during the last *c.* 10 kyr (see Supporting Information, Figure S5).

In terms of allelic diversity over a geographical space, the results from the Allelic Aggregation Index Analysis suggest a non-random, clumped distribution of alleles ($R = 0.00387$, $P < 0.001$). In Supporting Information, Figure S6, which is the Genetic Landscape Shape plot, the peaks represent the genetic distance between scorpions from different areas. This information indicates that the lowest genetic distance is found in the south-western part of *B. roigalsinai*'s distributional range (between Chañaral Island and the Choros region), with moderate genetic distances between populations towards the north, while the highest genetic distance can be found between Vicuña (VI) and neighbouring populations for *B. roigalsinai* and between neighbouring populations of *B. paposo* and *B. roigalsinai* (Llanos de Challe and Chañaral Island/Choros region). Considering the haplotype networks and distribution across space (Supporting Information, Figure S7), one can see that there are no shared mitochondrial haplotypes between the populations and that there is a clear separation between the two scorpion species regarding the similarities of the haplotype sequences. Within species the populations are generally structured as well, with a few exceptions such as the Choros region, where certain haplotypes are more similar to those from other populations than to their own. The nuclear haplotype networks display star-shaped patterns, reflecting a general lack of genetic structuring, especially for the actin fragment, where one haplotype is shared between four (non-adjacent) populations. Conversely, for wingless, one haplotype is present in all populations, a second haplotype is found only in *B. paposo* populations, and *B. roigalsinai*'s population from Vicuña has a unique haplotype, indicating a certain degree of geographical structuring. Similarly, from the graphs showing isolation-by-distance (Supporting Information, Figure S8), the overwhelming pattern is that genetic structuring by locality and geographic distance is only truly detectable in the mitochondrial gene fragment and, to a much lesser extent, in the wingless fragment, but not for actin.

The mutation-scaled effective population sizes (θ) and the mutation-scaled immigration rates (M) obtained from migrate-n are shown in Supporting Information (Table S7). Considering the mutation rates of the markers and assuming a generation time of 3 years, the effective population sizes were lowest for *B. roigalsinai*'s IC and VI, and *B. paposo*'s PP populations (approximate geometric means of 60703, 205092, and 595334, respectively) and highest for *B. paposo*'s PA and LC, and for *B. roigalsinai*'s CH populations (694718, 453813, and 595334, respectively), based on the geometric means of all markers. Based on the mitochondrial DNA, mean migration rates (in number of migrants per generation) were generally high between all adjacent populations of the same species (*B. paposo*'s PP and PA = 7.08×10^{-6}, *B. paposo*'s PA and LC = 9.94×10^{-6}, *B. roigalsinai*'s IC and CH = 9.25×10^{-6}, *B. roigalsinai*'s CH and VI = 6.12×10^{-6}), but lower between the populations from LC (*B. paposo*) and IC (*B. roigalsinai*) (mtDNA = 1.74×10^{-6}). This pattern is slightly different based on the wingless marker, where the lowest mean migration rate is between *B. roigalsinai*'s CH and VI populations (4.63×10^{-6}), followed by LC (*B. paposo*) and IC (*B. roigalsinai*) (3.99×10^{-6}), while the highest migration rates are between the conspecific populations PP and PA (7.49×10^{-6}), IC and CH (7.29×10^{-6}), and PA and LC (6.67×10^{-6}). The nuclear actin fragment shows no discernible pattern regarding inter- vs. intraspecific differences in mutation rates. The graphical outputs from the migrate-n runs can be found in Supporting Information, Figure S9.

The isolation-with-migration analyses in IMa2 estimated a very recent split between the *B. roigalsinai* populations from IC and CH (13 ka), and a 2.5 Ma split between these populations and VI, with estimated smaller ancestral than current populations. Also, migration between ancestral populations was not recovered as a possibility, estimating that the isolation between the population from VI and those from CH and IC occurred at their point of divergence. For *B. paposo,* on the other hand, the ancestral population size was estimated to be similar to current population sizes of PA and LC, while the population from PP is estimated to be smaller. Ancestral migrations were estimated between the MRCA of PA + LC and PP, as well as unsampled 'ghost' populations, although they were found not to be significant by the Nielsen & Wakeley test. The divergence between the LC and PA populations is estimated at 430 kya and at 2.5 Mya for the divergence of PP from LC+PA, with current migration rates similar to ancestral estimates (0.17, but not significant; see Supporting Information, Figure S10).

Bayesian phylogeography

The RRW phylogeographic analyses delimited the ancestral area of both *B. roigalsinai* and *B. paposo* approximately 4 Ma as almost the entire present-day area of distribution of the two species with 85%

highest posterior densities (HPD), encompassing the Chilean PCD between the latitudes of 30°S and 25.5°S. The 85% HPD polygons for the two species, representing the final separation of the ancestral areas in the sense of a definite end to gene flow, occurred approximately 400 kya, but never actually separated for each population (see Supporting Information, Figure S11).

DISCUSSION

The outcomes of this work redefine the geographic limits of the two species studied, with *B. paposo* being found in the northern localities of PP, PA and LC, and *B. roigalsinai* in IC, the adjacent mainland, CH and VI (Fig. 1). The new morphological diagnostic character presented here and used to definitively separate *B. roigalsinai* and *B. paposo* could be questioned, since the pigment pattern presents high variability in scorpions with wide distributions (such as *B. roigalsinai* and *B. paposo*) (Ojanguren-Affilastro, 2001, 2004); however, despite the overall high pigment variability of both species, in this particular case this character proved to be a strong and easily recognizable diagnostic character in all specimens examined.

In terms of geography, the two species appear to be separated by the Huasco River, with *B. roigalsinai*'s distributional range limited to the south by the Elqui River and *B. paposo*'s northern range by the Absolute Desert (Gajardo, 1993). This finding readjusts the distributional limits previously established, where *B. roigalsinai* was thought to extend further north (up to the northern limit of Atacama), and *B. paposo* to be endemic to the area of Paposo (Ojanguren-Affilastro, 2002; Ojanguren-Affilastro *et al.*, 2007a, b; Ojanguren-Affilastro & Pizarro-Araya, 2014).

The divergence time estimates for the species and each of their three populations varied, depending on the methods used, with the IMa2 age estimates being older than ages obtained with *BEAST, even though the confidence intervals in both cases were large and thus overlapped. Although the molecular clock rate of 0.0133 substitutions site^{-1} Myr^{-1} obtained for the mitochondrial fragment is higher than estimates previously obtained for COI in scorpions (e.g. 0.00925: Ceccarelli *et al.*, 2016; ; 0.007: Gantenbein *et al.*, 2005), the fact that a faster-evolving fragment (cyt *b*) was included here means that the rates obtained in this study are bound to be higher, and are therefore plausible.

The temporal congruence of the divergence of *B. paposo* and *B. roigalsinai*'s MRCA during the Pliocene, with the appearance of greater river flow from the Andes towards the Pacific (Turner *et al.*, 2005; Zemlak *et al.*, 2008), is strong evidence that the Huasco River acted as a barrier for the desert epigeic fauna, causing allopatric (vicariant) speciation in these scorpions. The time frame in which the River Huasco appears as a vicariant element for these scorpion species coincides with the end of the last, major uplift of the Andes, about 10–5 Mya, during which this mountain chain reached its present elevation (Ghosh, Garzione & Eiler, 2006; Garzione *et al.*, 2008). During this period, the medium and upper levels of the Andes began receiving a greater amount of snowfall coming from the humid air masses of the Pacific anticyclone. The melting of these snow masses increased the water flow of rivers such as the Huasco, which became permanent and exorheic, therefore creating an effective barrier for most of the epigeic arthropod fauna. A similar pattern of separation between coastal scorpion species is found between *Brachistosternus scioscia*e Ojanguren-Affilastro, 2002 and *Brachistosternus cepedai* Ojanguren-Affilastro, Agusto, Pizarro-Araya & Mattoni 2007, both with very similar morphology and habitat requirements (Ojanguren-Affilastro, 2002; Ojanguren-Affilastro *et al.*, 2007a, b), and both also separated by the Huasco river. The Copiapo river, on the other hand, is endorheic and with a comparatively reduced flow compared to the Huasco and Elqui rivers, and has therefore not acted as a barrier to gene flow for scorpions in the recent past.

An assessment of the genetic information used in this study reveals a general lack of structuring and poor phylogenetic resolution for the nuclear gene fragments, whereas there is greater resolution provided by the mitochondrial markers. This is probably due to the weaker phylo- and population genetic signal in nuclear than in mitochondrial markers, since the latter presumably have a higher mutation and coalescence rate, so they segregate sooner than the nuclear alleles. The overall low structuring may be due to past hybridisation events between the two species, if the barrier to gene flow (hypothesised as the River Huasco) disappeared during drier spells in geological history. This would be supported by the phylogeographic analysis, which only truly detects a separation of distributional ranges for the two species approximately 400 kya.

The relatively early point of separation between populations of *B. roigalsinai* from VI and CH obtained here by IMa2 (about 2.5 Ma, albeit with large confidence intervals) can be explained by the fact that Vicuña is located in the Precordillera, a low mountain range west of the Andes, whereas the Choros populations are found mainly in the coastal littoral plains. The intermediate area between these two populations is mostly covered by low mountains

and hills, which provide a suitable environment for *B. roigalsinai* only in some of its lowest, flattest areas. Therefore, this spatial fragmentation is likely to have promoted the isolation between the Choros and Vicuña populations. These events would also explain the high genetic distances detected in the Landscape Shape Plot of Alleles in Space between populations from these two localities.

The general population genetic trend revealed in this study, when comparing each of the three populations of *B. paposo* and *B. roigalsinai*, is that the three populations of the former show more genetic structuring and isolation, earlier divergence, higher mutation rates and less migration than *B. roigalsinai* populations. Nevertheless, it is difficult to say whether *B. paposo* populations underwent recent expansions after a bottleneck (as suggested by the population genetic parameters Tajima's D, Fu's F_S and $R_{2,}$ and by IMa2), since the extended Bayesian skyline plots (EBSP) showed stable population sizes during the last 500 kyr. However, given the shifts in suitable habitats due to sea-level changes, it is possible that populations may have been reduced in size by restricted available distributional ranges, thus undergoing genetic bottlenecks. In the case of *B. roigalsinai*, recent population expansion appears to have taken place in the population from VI, based on several independent lines of evidence (Tajima's D, Fu's F_S and R_2, and EBSP). For both species, the markers tested also revealed LD, which may be caused by mutation, random genetic drift, selection and/or gene flow, all of which would indicate some form of disturbance to the populations, most likely brought about by past environmental instability. Recent demographic expansion has been found in another desert scorpion (Graham *et al.*, 2013), suggesting that scorpions respond relatively quickly to localised environmental changes by moving their ranges. This is in contrast to other arachnid groups such as opilionids, which have been found to contain genetically highly structured populations, presumably due to their low vagility (Bragagnolo *et al.*, 2015; Clouse *et al.*, 2015).

The molecular evidence for low structuring and for events leading to depleted and unequal allelic diversity (as shown by the population genetic parameters as well as the clumped distribution detected by the Allelic Aggregation Index Analysis), further suggests relatively recent environmental instability, especially for *B. roigalsinai*, but also for *B. paposo*. In contrast to the apparent climatic stability of deserts such as the Atacama (Hartley *et al.*, 2005), coastal areas and habitats are affected by sea-level changes and in some cases tectonism (Pedoja *et al.*, 2014), immersing and emersing extended lowland areas, at times forming islands by immersing intermittent land to the mainland and with lower sea levels allowing the islands to reconnect. Such has been the fate also of Chañaral Island and the Choros archipelago, separated from the mainland by a present-day maximum seafloor depth of between 80–120 and 20–30 m, respectively. At times when the sea levels were therefore lower than these maximum depths, the islands were connected to the mainland and the populations of *B. roigalsinai* were able to interbreed in a generally larger area. The lack of genetic differences between the populations of *B. roigalsinai* of the Choros archipelago and the nearby mainland suggests that a connection of these islands to the continent existed until very recently. This is also reflected by the scarcity of morphological differences between island and continental specimens, and by the presence of similar scorpion communities in both areas (Pizarro-Araya *et al.*, 2014a).

Regarding the population from Chañaral island, the low structuring and lack of genetic diversity may be the result of a recent bottleneck following the island's separation from the mainland. The estimated 13 kyr of separation between the Chañaral island and Choros region populations coincides with the end of the last glacial maximum, during which the sea-level was about 100 m lower than today, thus exposing the intermittent seafloor. Despite the apparently short time span of separation between the Chañaral and continental populations of *B. roigalsinai*, island specimens are about 30% smaller than continental specimens, and much more densely pigmented (Pizarro-Araya *et al.,* MS in prep.). This reduction in size has been documented in other insular organisms (especially well studied in mammals) which commonly display the phenomenon of gigantism or dwarfism, also termed the 'island rule' (Van Valen, 1973). Williams (1980) and later Polis (1990) refer to some cases of gigantism in scorpions in islands of Baja California; Williams (1980) states that 'these size variations are probably best explained by differences in prey availability in various habitats'. This finding could also explain the smaller average size of *B. roigalsinai* of Chañaral island, where in a recent biological inventory of the epigeic insects, Pizarro-Araya *et al.* (2014a, b) discovered a remarkably lower species richness compared to the continent. This represents an impoverishment in prey availability for scorpions on the island, since they feed mainly on epigeic arthropods.

Comparing and contrasting Chañaral island and the Choros archipelago, it is noteworthy that *B. roigalsinai* is the only scorpion species present on the former, in contrast to the rich scorpion communities found on the latter. Differences in both island communities could be explained either by their different histories, since both present almost identical

environmental conditions and landmasses, and/or by the effect of different ecological communities present on the islands. Another point to note is that while Chañaral island harbours one endemic species of spider of the family Zodariidae (Grismado & Pizarro-Araya, 2016), and the Choros archipelago contains one endemic coleopteran of the family Tenebrionidae, *Gyriosomus granulipennis* (Pizarro-Araya & Flores, 2004; Alfaro, Pizarro-Araya & Flores, 2009) there is a lack of endemic scorpion species on these islands. This is probably a result of the high vagility of the scorpions of the area and their lower ecological/genetic constraints compared to other epigeic arthropods. In fact, most scorpions from these islands can be considered stenotopic species, that can survive in a wide range of environments (Agusto *et al.*, 2006; Pizarro-Araya *et al.*, 2014a). Another plausible, and possibly concurrent, explanation could be the different reproductive strategies presented by the endemic arthropods compared to scorpions. Most arthropods are typical r strategists, presenting a large number of offspring, high growth rate and short generation times (i.e. life span), all of which favour higher speciation rates. Conversely, field data (J. Pizarro pers. obs.) reveal that both scorpion species studied here are typical K strategists (Wallwork, 1982), like many other desert scorpions (Warburg & Polis, 1990), with fewer offspring, a lower growth rate, and longer generation times (hence lower speciation rates) meaning that it would take longer for scorpions to speciate into island endemics.

In summary, the Chilean coastal desert, including its continental-shelf islands, harbours species which have had to adapt to a coastline habitat that is constantly changing due to sea-level oscillations and tectonics, by moving. This geological instability is reflected in the present population genetic and phylogeographic studies by the general low genetic diversity and apparent recent diversification of the populations. The insular populations, although only recently separated, already show some degree of differentiation, while perhaps more striking is the vicariant effect of the Huasco River on the two species, *B. paposo* and *B. roigalsinai*. So while this river, and to a certain degree the inland hills have played a role in separating and structuring populations, eustasy is likely to have had a destabilizing effect on coastal populations.

ACKNOWLEDGEMENTS

Our acknowledgements to CONAF (Corporación Nacional Forestal, Chile) for helping us obtain permission and providing facilities to work in the SNASPE areas (Projects No. 006/2014 and 028/2015). This study was funded by the DIULS PR13121 and PR15121/VACDDI001 projects of the University of La Serena, La Serena, Chile (JPA), PICT 2010-764, PICT 2011-1007 and iBol (Arg.) 2012 to AAOA, and a postdoctoral grant from CONICET (Consejo Nacional de Investigaciones Científicas y Técnicas, Argentina) to FSC. We also thank A. Sánchez-Gracia, A. Martínez-Aquíno and N. Trujillo-Arias for advice on population genetic analyses and E. González-Santillán and three anonymous referees for comments which helped improve the manuscript. We are especially indebted to Fermín Alfaro, Juan Enrique Barriga-Tuñón, Ricardo Botero-Trujillo, Luis Compagnucci, Camilo Mattoni, Pablo Agusto, Jose Mondaca, Hernán Iuri, Carolina Cuezzo, Alberto Castex, Juan Campusano, Cristian Rivera (CONAF-Atacama, Chañaral Island), Patricio Ortiz (Aljavig), Paula Martinez and Pablo Arróspide (CONAF-Coquimbo) for their invaluable help during the collecting trips.

REFERENCES

Aguirre L. 1967. Geología de las islas Choros, Damas y de Punta Choros, Provincia de Coquimbo. *Revista Minerales (Chile)* **22:** 73–83.

Agusto P, Mattoni CI, Pizarro-Araya J, Cepeda-Pizarro J, López-Cortés F. 2006. Comunidades de escorpiones (Arachnida: Scorpiones) del desierto costero transicional de Chile. *Revista Chilena de Historia Natural* **79:** 407–421.

Alfaro FM, Pizarro-Araya J, Flores GE. 2009. Epigean tenebrionids (Coleoptera: Tenebrionidae) from the Choros archipelago (Coquimbo Region, Chile). *Entomological News* **120:** 125–130.

Alfaro FM, Pizarro-Araya J, Mondaca J. 2014. New insular records of *Germarostes* (*Germarostes*) *posticus* (Germar) (Coleoptera, Hybosoridae, Ceratocanthinae) for the chilean transitional coastal desert. *Coleopterist Bulletin* **68:** 387–390.

Beerli P. 2006. Comparison of Bayesian and maximum-likelihood inference of population genetic parameters. *Bioinformatics* **22:** 341–345.

Beerli P. 2009. How to use MIGRATE or why are Markov chain Monte Carlo programs difficult to use. In: Bertorelle Giorgio, Bruford MW, Hauffe, Heidi C, Rizzoli A, Vernesi C, eds. *Population Genetics for Animal Conservation*. Cambridge, UK: Cambridge University Press, 42–79.

Benítez HA, Pizarro-Araya J, Bravi R, Sanzana MJ, Alfaro FM. 2014. Morphological variation on isolated populations of *Praocis* (*Praocis*) *spinolai*. *Journal of Insect Science* **14:** 11.

Bielejec F, Rambaut A, Suchard MA, Lemey P. 2011. SPREAD: spatial phylogenetic reconstruction of evolutionary dynamics. *Bioinformatics* **27:** 2910–2912.

Blackledge TA, Scharff N, Coddington JA, Szüts T, Wenzel JW, Hayashi CY, Agnarsson I. 2009. Reconstructing web evolution and spider diversification in the

molecular era. *Proceedings of the National Academy of Sciences* **106:** 5229–5234.

Bodner MR, Maddison WP. 2012. The biogeography and age of salticid spider radiations (Araneae: Salticidae). *Molecular Phylogenetics and Evolution* **65:** 213–240.

Boulton AM, Polis GA. 1990. Phenology and life history of the desert spider, *Diguetia mojavea* (Araneae, Diguetidae). *The Journal of Arachnology* **27:** 513–521.

Bragagnolo C, Pinto-da-Rocha R, Antunes M Jr, Clouse RM. 2015. Phylogenetics and phylogeography of a long-legged harvestman (Arachnida: Opiliones) in the Brazilian Atlantic Rain Forest reveals poor dispersal, low diversity and extensive mitochondrial introgression. *Invertebrate Systematics* **29:** 386–404.

Bryson RW Jr, Savary WE, Prendini L. 2013. Biogeography of scorpions in the *Pseudouroctonus minimus* complex (Vaejovidae) from south-western North America: implications of ecological specialization for pre-quaternary diversification. *Journal of Biogeography* **40:** 1850–1860.

Carter RWG. 1988. *Coastal Environments: An Introduction to the Physical*. Ecological and Cultural Systems of Coastlines: Academic Press, London, UK.

Castro C, Brignardello L. 2005. Geomorfología aplicada a la ordenación territorial de litorales arenosos. Orientaciones para la protección, usos y aprovechamiento sustentables del sector de Los Choros, Comuna de La Higuera, IV Región. *Revista de Geografía Norte Grande* **33:** 33–58.

Ceccarelli FS, Ojanguren-Affilastro AA, Ramírez MJ, Ochoa JA, Mattoni CI, Prendini L 2016. Andean uplift drives diversification of the bothriurid scorpion genus *Brachistosternus*. *Journal of Biogeography*. doi:10.1111/jbi.12760.

Clouse RM, Sharma PP, Stuart JC, Davis LR, Giribet G, Boyer SL, Wheeler WC. 2015. Phylogeography of the harvestman genus Metasiro (Arthropoda, Arachnida, Opiliones) reveals a potential solution to the Pangean paradox. *Organisms Diversity and Evolution* **16:** 167–184.

Drummond AJ, Suchard MA, Xie D, Rambaut A. 2012. Bayesian phylogenetics with BEAUti and the BEAST 1.7. *Molecular Biology and Evolution* **29:** 1969–1973.

Fu YX. 1997. Statistical tests of neutrality of mutations against population growth, hitchhiking and background selection. *Genetics* **147:** 915–925.

Gajardo R. 1993. *La vegetación natural de Chile*. Santiago, Chile: Editorial Universitaria.

Gantenbein B, Fet V, Gantenbein-Ritter IA, Balloux F. 2005. Evidence for recombination in scorpion mitochondrial DNA (Scorpiones: Buthidae). *Proceedings of the Royal Society B: Biological Sciences* **272:** 697–704.

Garzione CN, Hoke GD, Libarkin JC, Withers S, MacFadden B, Eiler J, Ghosh P, Mulch A. 2008. Rise of the Andes. *Science* **320:** 1304–1307.

Ghosh P, Garzione CN, Eiler JM. 2006. Rapid uplift of the Altiplano revealed through 13C–18O bonds in paleosol carbonates. *Science* **311:** 511–515.

Graham MR, Oláh-Hemmings V, Fet V. 2012. Phylogeography of co-distributed dune scorpions identifies the Amu Darya River as a long-standing component of Central Asian biogeography. *Zoology in the Middle East* **55:** 95–110.

Graham MR, Jaeger JR, Prendini L, Riddle BR. 2013. Phylogeography of Beck's Desert Scorpion, *Paruroctonus becki*, reveals Pliocene diversification in the Eastern California Shear Zone and postglacial expansion in the Great Basin Desert. *Molecular Phylogenetics and Evolution* **69:** 502–513.

Grismado CJ, Pizarro-Araya J. 2016. On the spider genus *Cyrioctea* Simon on Isla Chañaral (Pingüino de Humboldt National Reserve, Atacama, Chile): Description of a new species, and description of the male of *Cyrioctea cruz* Platnick (Araneae, Zodariidae). *Zootaxa* **4107:** 267–276.

Guillot G, Santos F. 2009. A computer program to simulate multilocus genotype data with spatially auto-correlated allele frequencies. *Molecular Ecology Resources* **9:** 1112–1120.

Haq BU, Hardenbol J, Vail PR. 1988. Mesozoic and Cenozoic chronostratigraphy and cycles of sea level change. In: Wilgus CK, Hastings BS, Kendall CGSt, Posamentier HW, Ross CA, Van Wagoner JC, eds. *Sea level changes: an integrated approach*. Tulsa, OK: Society of Economic Paleontologists and Mineralogists Special Publication **42:** 71–108.

Hardenbol J, Thierry J, Farley MB, Jacquin T, Graciansky P-C, Vial PR 1998. Mesozoic and Cenozoic sequence chronostratigraphic framework of European basins. In: Graciansky P-C, Hardenbol J, Jacquin T, Vail PR eds., *Mesozoic and Cenozoic Sequence Stratigraphy of European Basins SEPM*, Tulsa, OK: Special Publication 60: Chart 1, 3–13.

Hartley AJ, Chong G, Houston J, Mather AE. 2005. 150 million years of climatic stability: evidence from the Atacama Desert, northern Chile. *Journal of the Geological Society, London* **162:** 421–424.

Heled J, Drummond AJ. 2008. Bayesian inference of population size history from multiple loci. *BMC Evolutionary Biology* **8:** 289.

Heled J, Drummond AJ. 2010. Bayesian inference of species trees from multilocus data. *Molecular Biology and Evolution* **27:** 570–580.

Hey J. 2010. Isolation with migration models for more than two populations. *Molecular Biology and Evolution* **27:** 905–920.

Hey J, Nielsen R. 2007. Integration within the Felsenstein equation for improved Markov chain Monte Carlo methods in population genetics. *Proceedings of the National Academy of Sciences* **104:** 2785–2790.

Hudson RR. 1987. Estimating the recombination parameter of a finite population model without selection. *Genetics Research* **50:** 245–250.

Hudson RR. 1990. Gene genealogies and the coalescent process. *Oxford Surveys in Evolutionary Biology* **7:** 1–44.

Hudson RR, Kaplan NL. 1985. Statistical properties of the number of recombination events in the history of a sample of DNA sequences. *Genetics* **111:** 147–164.

Huelsenbeck JP, Andolfatto P. 2007. Inference of population structure under a Dirichlet process model. *Genetics* **175:** 1787–1802.

Huelsenbeck JP, Andolfatto P, Huelsenbeck ET. 2011. Structurama: Bayesian inference of population structure. *Evolutionary Bioinformatics* **7:** 55.

Husson L, Conrad CP, Faccenna C. 2012. Plate motions, Andean orogeny, and volcanism above the South Atlantic convection cell. *Earth and Planetary Science Letters* **317–318:** 126–135.

Jensen JL, Bohonak AJ, Kelley ST. 2005. Isolation by distance, web service. BMC Genetics 6: 13. v.3.23 http://ibdws.sdsu.edu/

Jukes TH, Cantor CR. 1969. *Evolution of protein molecules*. New York: Mammalian Protein Metabolism Academic Press, 21–132.

Katoh K, Standley DM. 2013. MAFFT multiple sequence alignment software version 7: improvements in performance and usability. *Molecular Biology and Evolution* **30:** 772–780.

Kelly JK. 1997. A test of neutrality based on interlocus associations. *Genetics* **146:** 1197–1206.

Kendrick E, Bevis M, Smalley RJ, Brooks B, Vargas RB, Lauría E, Fortes LPS. 2003. The Nazca-South America Euler vector and its rate of change. *Journal of South American Earth Sciences* **16:** 125–131.

Kovařík F, Ojanguren-Affilastro AA. 2013. *Illustrated catalog of scorpions. Part II. Bothriuridae; Chaerilidae; Buthidae I., genera Compsobuthus, Hottentotta, Isometrus, Lychas, and Sassanidotus*. Czech Republic: Jakub Rolčík Publisher, 400.

Lanfear R, Calcott B, Ho SYW, Guindon S. 2012. PartitionFinder: combined selection of partitioning schemes and substitution models for phylogenetic analyses. *Molecular Biology and Evolution* **29:** 1695–1701.

Le Roux JP, Gómez C, Venegas C, Fenner J, Middleton H, Marchant M, Buchbinder B, Frassinetti D, Marquardt C, Gregory-Wodzicki KM, Lavenu A. 2005. Neogene-Quaternary coastal and offshore sedimentation in north central Chile: Record of sea-level changes and implications for Andean tectonism. *Journal of South American Earth Sciences* **19:** 83–98.

Leigh JW, Bryant D. 2015. POPART: full-feature software for haplotype network construction. *Methods in Ecology and Evolution* **6:** 1110–1116.

Lemey P, Rambaut A, Welch JJ, Suchard MA. 2010. Phylogeography takes a relaxed random walk in continuous space and time. *Molecular Biology and Evolution* **27:** 1877–1885.

Librado P, Rozas J. 2009. DnaSP v5: a software for comprehensive analysis of DNA polymorphism data. *Bioinformatics* **29:** 1451–1452.

Lynch M, Crease TJ. 1990. The analysis of population survey data on DNA sequence variation. *Molecular Biology and Evolution* **7:** 377–394.

Maddison WP, Maddison DR. 2015. Mesquite: a modular system for evolutionary analysis. Version 3.04 http://mesquiteproject.org.

Manel S, Schwartz ML, Luikart G, Taberlet P. 2003. Landscape genetics: combining landscape ecology and population genetics. *Trends in Ecology and Evolution* **18:** 189–197.

Mantel N. 1967. The detection of disease clustering and a generalized regression approach. *Cancer Research* **27:** 209–220.

Miller MP. 2005. Alleles in space (ais): computer software for the joint analysis of interindividual spatial and genetic information. *Journal of Heredity* **96:** 722–724.

Miller MP, Bellinger MR, Forsman ED, Haig SM. 2006. Effects of historical climate change, habitat connectivity, and vicariance on genetic structure and diversity across the range of the red tree vole (*Phenacomys longicaudus*) in the Pacific Northwestern United States. *Molecular Ecology* **15:** 145–159.

Miller MA, Pfeiffer W, Schwartz T. 2010. Creating the CIPRES Science Gateway for inference of large phylogenetic trees. Pp. 1–8 in Proceedings of the Gateway Computing Environments Workshop (GCE), 14 Nov. 2010, New Orleans, LA.

Mirshamsi O, Sari A, Elahi E, Hosseini S. 2010. Phylogenetic relationships of *Mesobuthus eupeus* (C.L. Koch, 1839) inferred from *COI* sequences (Scorpiones: Buthidae). *Journal of Natural History* **44:** 2851–2872.

Mulroy TW, Rundel PW. 1977. Adaptations to desert environments. *BioScience* **27:** 109–114.

Nagy KA. 2004. Water economy of free-living desert animals. *International Congress Series* **1275:** 291–297.

Nei M. 1987. *Molecular evolutionary genetics*. New York: Columbia University Press.

Nielsen R, Wakeley J. 2001. Distinguishing migration from isolation: a Markov chain Monte Carlo approach. *Genetics* **158:** 885–896.

Nylinder S, Lemey P, De Bruyn M, Suchard MA, Pfeil BE, Walsh N, Anderberg AA. 2014. On the biogeography of Centipeda: a species-tree diffusion approach. *Systematic Biology* **63:** 178–191.

Ochoa JA. 2005. Patrones de distribución de escorpiones de la región andina en el sur peruano. *Revista Peruana de Biología* **12:** 49–68.

Ojanguren-Affilastro AA. 2001. Sistemática y distribución de *Brachistosternus alienus* Lönnberg (Scorpiones; Bothriuridae). *Revista del Museo Argentino de Ciencias Naturales, Nueva Serie* **3**(2)**:** 169–174.

Ojanguren-Affilastro AA. 2002. Nuevos aportes al conocimiento del género *Brachistosternus* en Chile, con la descripción de dos nuevas especies (Scorpiones, Bothriuridae). *Boletín de la Sociedad de Biología de Concepción (Chile)* **73:** 37–46.

Ojanguren-Affilastro AA. 2004. Sistemática y distribución de *Brachistosternus (Leptosternus) intermedius* Lönnberg (Scorpiones; Bothriuridae). *Physis* (Buenos Aires), Sección C **59**(136–137)**:** 29–35.

Ojanguren-Affilastro AA, Pizarro-Araya J. 2014. Two new scorpion species from Paposo, in the Coastal desert of Taltal, Chile (Scorpiones, Bothriuridae, *Brachistosternus*). *Zootaxa* **3785:** 400–418.

Ojanguren-Affilastro AA, Ramírez MJ. 2009. Phylogenetic analysis of the scorpion genus *Brachistosternus* (Arachnida, Scorpiones, Bothriuridae). *Zoologica Scripta* **38:** 183–198.

Ojanguren-Affilastro AA, Mattoni CI, Prendini L. 2007a. The genus *Brachistosternus* (Scorpiones: Bothriuridae) in Chile, with descriptions of two new species. *American Museum Novitates* **3564:** 1–44.

Ojanguren-Affilastro AA, Agusto P, Pizarro-Araya J, Mattoni CI. 2007b. Two new scorpion species of genus *Brachistosternus* (Scorpiones: Bothriuridae) from northern Chile. *Zootaxa* **1623:** 55–68.

Ojanguren-Affilastro AA, Mattoni CI, Ochoa JA, Ramírez MJ, Ceccarelli FS, Prendini L. 2016. Phylogeny, species delimitation and convergence in the South American bothriurid scorpion genus *Brachistosternus* Pocock 1893: Integrating morphology, nuclear and mitochondrial DNA. *Molecular Phylogenetics and Evolution* **94:** 159–170.

Pedoja K, Husson L, Johnson ME, Melnick D, Witt C, Pochat S, Nexer M, Delcaillau B, Pinegina T, Poprawski Y, Authemayou C, Elliot M, Regard V, Garestier F. 2014. Coastal staircase sequences reflecting sea-level oscillations and tectonic uplift during the Quaternary and Neogene. *Earth-Science Reviews* **132:** 13–38.

Pizarro-Araya J, Flores GE. 2004. Two new species of *Gyriosomus* Guérin-Méneville from Chilean coastal desert (Coleoptera: Tenebrionidae: Nycteliini). *Journal of the New York Entomological Society* **112:** 121–126.

Pizarro-Araya J, Agusto P, López-Cortes F, Ojanguren-Affilastro AA, Briones R, Cepeda-Pizarro J. 2014a. Diversidad y composición estacional de la escorpiofauna (Arachnida: Scorpiones) del archipiélago Los Choros (Región de Coquimbo, Chile). *Gayana* **78:** 46–56.

Pizarro-Araya J, Alfaro FM, Cortés-Contreras M, Rivera C, Vargas-Talciani P, Ojanguren-Affilastro AA. 2014b. Epigean Insects of Chañaral Island (Pingüino de Humboldt National Reserve, Atacama, Chile). *Journal of the Entomological Research Society* **16:** 39–50.

Polis GA. 1990. *The biology of scorpions*. Stanford University Press, Stanford, CA.

Polis GA, Farley RD. 1980. Population biology of a desert scorpion: survivorship, microhabitat, and the evolution of life history strategy. *Ecology* **61:** 620–629.

R Core Team. 2014. R: A Language and Environment for Statistical Computing. R Foundation for Statistical Computing, Vienna. https://www.R-project.org.

Rambaut A, Suchard M, Xie W, Drummond A. 2014. Tracer v. 1.6. Institute of Evolutionary Biology, University of Edinburgh.

Ramos-Onsins SE, Rozas J. 2002. Statistical properties of new neutrality tests against population growth. *Molecular Biology and Evolution* **19:** 2092–2100.

Stephens M, Donnelly P. 2003. A comparison of Bayesian methods for haplotype reconstruction from population genotype data. *The American Journal of Human Genetics* **73:** 1162–1169.

Stephens M, Smith NJ, Donnelly P. 2001. A new statistical method for haplotype reconstruction from population data. *The American Journal of Human Genetics* **68:** 978–989.

Tajima F. 1989. Statistical method for testing the neutral mutation hypothesis by DNA polymorphism. *Genetics* **123:** 585–595.

Tamura K, Stecher G, Peterson D, Filipski A, Kumar S. 2013. MEGA6: Molecular Evolutionary Genetics Analysis Version 6.0. *Molecular Biology and Evolution* **30:** 2725–2729.

Templeton AR, Crandall KA, Sing CF. 1992. A cladistic analysis of phenotypic associations with haplotypes inferred from restriction endonuclease mapping and DNA sequence data. *III. Cladogram estimation. Genetics.* **132:** 619–633.

Turner KJ, Fogwill CJ, McCulloch RD, Sugden DE. 2005. Deglaciation of the eastern flank of the North Patagonian Icefield and associated continental-scale lake diversions. *Geografiska Annaler Series A: Physical Geography* **87A:** 363–374.

Van Valen L. 1973. A new evolutionary law. *Evolutionary Theory* **1:** 1–33.

Vink CJ, Hedin M, Bodner MR, Maddison WP, Hayashi CY, Garb JE. 2008. Actin 5C, a promising nuclear gene for spider phylogenetics. *Molecular Phylogenetics and Evolution* **48:** 377–382.

Wallwork JA. 1982. *Desert Soil Fauna*. Santa Barbara, CA: Praeger Publishers Inc.

Warburg MR, Polis GA. 1990. Behavioral responses, rhythms and activity patterns. In: Polis GA, ed. *The Biology of Scorpions: 224–246*. Redwood City, CA: Stanford University Press, 587.

Watterson GA. 1975. On the number of segregating sites in genetical models without recombination. *Theoretical Population Biology* **7:** 256–276.

Whitford WG. 2002. *Ecology of Desert Systems*. Elsevier, London, UK: Academic Press.

Williams SC. 1980. Scorpions of Baja California, Mexico and Adjacent Islands. Occasional Papers of the California Academy of Science. **135:** 1–127.

Wright S. 1931. Evolution in mendelian populations. *Genetics* **16:** 97–159.

Zemlak TS, Habit EM, Walde SJ, Battini MA, Adams EDM, Ruzzante DE. 2008. Accross the southern Andes on fin: Glacial refugia, drainage reversals and a secondary contact zone revealed by the phylogeographical signal of *Galaxias platei* in Patagonia. *Molecular Ecology* **17:** 5049–5061.

SUPPORTING INFORMATION

Additional Supporting Information may be found online in the supporting information tab for this article:

Figure S1. Map showing the SNASPE Pingüino de Humboldt National Reserve.
Figure S2. Geneland heat maps.

Figure S3. Geneland and Structurama probabilities for number of populations.
Figure S4. NJ trees from Dxy/a calculations.
Figure S5. Extended Bayesian skyline plots.
Figure S6. Alleles-In-Space landscape plot.
Figure S7. TCS haplotype networks and maps.
Figure S8. Isolation-by-distance graphs.
Figure S9. migrate-n graphical outputs.
Figure S10. IMa2 figures.
Figure S11. Google Earth time slices of relaxed random walk phylogeographic analysis.
Table S1. Individual specimens, sampling locality numbers, and GenBank accession numbers for *Brachistosternus paposo* and *Brachistosternus roigalsinai*.
Table S2. Primers used for amplification of molecular markers.
Table S3. Partitioning strategy and nucleotide substitution models for phylogenetic analices.
Table S4. Specifications of data matrices for gene fragments used in molecular analyses.
Table S5. Results of neutrality and LD tests.
Table S6. F_{st} and D_{xy}/D_a calculations.
Table S7. Migrate-n Bayesian posterior distribution values.